



Lawrence Berkeley Laboratory

UNIVERSITY OF CALIFORNIA

Accelerator & Fusion Research Division

Invited paper presented at the Fourteenth International Free
Electron Laser Conference, Kobe, Japan, August 23-28, 1992,
and to be published in the Proceedings

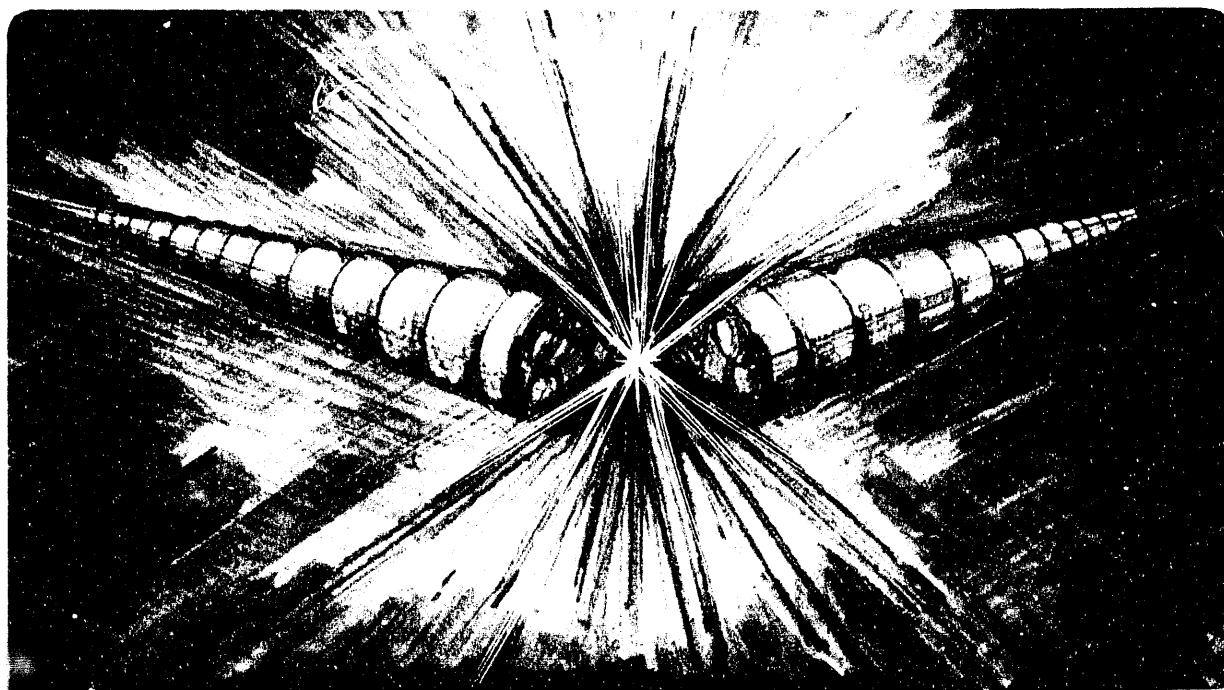
Self-Amplified Spontaneous Emission for Short Wavelength Coherent Radiation

K.-J. Kim and M. Xie

September 1992

Received by OSTI

DEC 21 1992



Prepared for the U.S. Department of Energy under Contract Number DE-AC03-76SF00098

DISTRIBUTION OF THIS DOCUMENT IS UNLIMITED

DISCLAIMER

This document was prepared as an account of work sponsored by the United States Government. Neither the United States Government nor any agency thereof, nor The Regents of the University of California, nor any of their employees, makes any warranty, express or implied, or assumes any legal liability or responsibility for the accuracy, completeness, or usefulness of any information, apparatus, product, or process disclosed, or represents that its use would not infringe privately owned rights. Reference herein to any specific commercial product, process, or service by its trade name, trademark, manufacturer, or otherwise, does not necessarily constitute or imply its endorsement, recommendation, or favoring by the United States Government or any agency thereof, or The Regents of the University of California. The views and opinions of authors expressed herein do not necessarily state or reflect those of the United States Government or any agency thereof or The Regents of the University of California and shall not be used for advertising or product endorsement purposes.

Lawrence Berkeley Laboratory is an equal opportunity employer.

Self-Amplified Spontaneous Emission for Short Wavelength Coherent Radiation*

Kwang-Je Kim and Ming Xie

Lawrence Berkeley Laboratory
University of California
Berkeley, CA 94720

Abstract:

We review the recent progress in our understanding of the self-amplified spontaneous emission (SASE), emphasizing the application to short wavelength generation. Simple formulae are given for the start-up, exponential gain and the saturation of SASE. Accelerator technologies producing high brightness electron beams required for short wavelength SASE are discussed. An example utilizing electron beams from a photocathode-linac system to produce 4nm SASE in the multigigawatt range is presented.

Invited paper presented at the 14th International FEL Conference, Kobe, Japan, 23-28 August, 1992

- * This work was supported by the Director, Office of Energy Research, Office of Basic Energy Sciences, Materials Sciences Division, of the U.S. Department of Energy under Contract No. DE-AC03-76SF00098.

MASTER

1. Introduction

When an electron beam with sufficiently high intensity and brightness passes through a long undulator, the interaction between radiation and electron beam leads to an exponential amplification of the spontaneous emission, giving rise to high power, coherent radiation at the end of the undulator. This so-called self-amplified spontaneous emission (SASE) is attractive as a source of high-power, coherent radiation in wavelength region shorter than 1000 Å, where high reflectivity mirrors are not available and thus the usual free-electron lasers (FELs) utilizing optical resonators cannot be operated. This paper is a review of the recent progress in the understanding of SASE.

The interest in SASE began with a clear discussion of the exponential gain regime of FEL by Bonifacio, Pellegrini and Narducci [1], and the suggestion by Pellegrini on use of SASE as a coherent, high-power radiation source [2]. These authors emphasized the importance of a dimensionless strength parameter, sometimes known as the Pierce parameter, ρ , in understanding high gain FELs. The parameter ρ is defined by

$$\rho = \left(\frac{e^2 Z_0 n K^2 [JJ]}{32 \gamma^3 m c^2 k_u^2} \right)^{1/3}, \quad (1)$$

where e is the electron charge, $Z_0 = 377 \Omega$, n is the peak electron density, m is electron mass, c is speed of light, γ is the electron energy in units of mc^2 , $k_u = 2\pi/\lambda_u$, λ_u is the period length of undulator magnet, $K = e B_0/(k_u mc)$, B_0 is the peak magnetic field of the undulator, and $[JJ]$ is the usual factor involving Bessel functions. By analyzing 1-D models, they found that the gain and saturation characteristics are determined by ρ . In particular, the saturated optical power level is given approximately by ρ times the electron beam kinetic power.

The actual evolution of the initial spontaneous emission into an exponentially growing coherent radiation was studied by means of the coupled Maxwell-Vlasov equations in 1-D model by Kim [3], and by Wang and Yu [4]. The study clarified the nature of SASE evolution, and determined the amount of the equivalent input noise power.

The 1-D calculation of the growth rate was generalized to include the 3-D property of the radiation (diffraction) but neglecting the electron beam focusing effect in ref. [5] and [6].

Attempt to analytically determine the growth rate including the effects due to diffraction, electron beam focusing and energy spread was started in ref. [7], where an eigenvalue equation for electromagnetic field was derived. The equation was solved by variational method [8] for a waterbag model of electron beam distribution. For a general distribution, a perturbation theory of the Maxwell-Vlasov equation was developed recently [9].

The basic concept of SASE was demonstrated experimentally in the microwave region at LLNL [10]. An experimental realization of SASE in the short wavelength region has been slow due to the challenging requirement on electron beam characteristics. There has been extensive discussion of using a special bypass of a storage ring [11]. Recently, the use of linacs are actively discussed [12] due to the development of high-brightness RF photocathodes [13]. It appears that SASE based on such accelerators are a promising way to generate multi-gigawatts of coherent power in the "water window" region.

2. Start-Up From Noise

The evolution of the SASE power is schematically illustrated in Fig. 1. After an initial region, sometimes called the lethargy region, where the power grows linearly with distance, the power spectrum grows exponentially as follows:

$$\frac{dP}{d\omega} = e^{z/L_G} S(\omega, z) \left(\frac{dP}{d\omega} \right)_{\text{noise}}, \quad (2)$$

where L_G is the power gain length, $S(\omega, z)$ is a function describing the frequency dependence of the gain, and $(dP/d\omega)_{\text{noise}}$ is the noise power spectrum due to the spontaneous emission. The noise power spectrum was calculated in 1-D model [3], [4], and can be expressed in the following form [7]:

$$\left(\frac{dP}{d\omega} \right)_{\text{noise}} = \frac{\rho E_0}{2\pi}, \quad (3)$$

where $E_0 = mc^2\gamma_0$ is the energy of a single electron. This power can be interpreted [15] as the spontaneous power emitted in one gain length L_G^{1-D} in 1-D theory

$$L_G^{1-D} = 1/2\sqrt{3}\rho k_u \quad (4)$$

Krinsky and Yu have considered the modification of Eq. (3) in the presence of 3-D effects [14].

Note that Eq. (3) describes a white noise spectrum. The frequency spectrum of the amplified radiation is determined by the factor $S(\omega, z)$ in Eq. (2), the bandwidth of which is approximately given by

$$\frac{\Delta\omega}{\omega} \sim \sqrt{\frac{\rho}{N}} \quad (5)$$

where $N = z/\lambda_u$ is the number of the undulator periods in z .

3. Exponential Growth

The electromagnetic field amplitude A and the perturbation of the electron distribution function δf are coupled linearly through the Maxwell and Vlasov equations. The growth rate is obtained by assuming that A and δf are proportional to $\exp(-i k_u \tilde{\mu} z)$ and solving for $\tilde{\mu}$. In 1-D theory, this can be done analytically. One finds that the imaginary part μ of $\tilde{\mu}$ for vanishing electrons' momentum spread is given by $\sqrt{3}\rho$, leading to the 1-D power gain length $L_G^{1-D} = 1/(2\sqrt{3} k_u \rho)$. Including the 3-D diffraction effect [5], [6] and the electrons' betatron motion [8], [9], the gain will be reduced. However, the reduction is small if

$$2 k \epsilon_x \lesssim 1 \quad (6)$$

$$L_G^{1-D}/L_R \lesssim 1 \quad (7)$$

$$\sigma_\gamma/\gamma < \rho \quad (8)$$

Here $k = \omega/c = 2\pi/\lambda$ is the radiation wave number, ϵ_x is the rms electron beam emittance (considered the same in the x and y plane), and L_R is the Raleigh length defined by $L_R = 2k\langle x^2 \rangle = 2k \epsilon_x \beta$, where β is the value of the betatron function, and σ_γ is the rms energy

spread. The inequality (6) can be obtained by comparing the emittance of the electron beam with that of the TEM_{00} mode [15]. The inequality (7) is the statement that diffraction is not important in one gain length [16]. The inequality (8) can be obtained from the fact that the gain bandwidth of high gain FEL is about ρ .

Including 3-D effect and electrons' betatron motion, the equations become too complicated for exact analytical solution. Two methods have been developed to obtain an approximate solution. In the first, the Vlasov equation was solved by the technique of integrating over unperturbed trajectories. The result is inserted to the Maxwell equation which now become an eigenvalue problem involving the electromagnetic field only [7]. In the particular case where the unperturbed electron distribution function is given by the waterbag model, the eigenvalue equation could be solved by a variational technique [8]. The growth rate so obtained was found to agree well with that obtained numerically from simulation code.

In the second approach [9], one first solve the Maxwell equation using the Green's function technique, and the result is inserted to the Vlasov's equation to obtain an eigenvalue equation involving δf only. The equation is solved by expanding δf in terms of a complete set of orthogonal functions in electron phase space. The lowest order dispersion relation obtained by neglecting coupling to higher order modes is as follows:

$$1 + 16 \frac{k^2 \rho^3 \Sigma}{\pi} \int_0^\infty dR^2 R^2 F(R) \frac{V(\eta) d\eta}{\left(\tilde{\mu} + 2\eta - \frac{k R^2}{2 k_u \beta^2} \right)^2} \times \int \frac{\theta d\theta}{\left(\tilde{\mu} + \Delta v + \frac{k \theta^2}{2 k_u} \right)} \left[\int R^2 dR^2 F(R) \frac{J_1(kR\theta)}{kR\theta} \right]^2 = 0 \quad , \quad (9)$$

where $F(R)$ is the unperturbed transverse distribution function of electrons, normalized so that $\int F(R) R^2 dR^2 = 1$, the variable R being the betatron amplitude: $R^2 = x^2 + \beta^2 x'^2$, where $x =$

transverse coordinate, x' = transverse angle and β is the magnitude of the betatron function, $V(\eta)$ is the distribution of the relative momentum of electrons, normalized so that $\int V(\eta)d\eta = 1$,

Σ is the cross sectional area of the electron beam (so that $n\Sigma$ is the linear density), and

$\Delta\nu = (\omega - \omega_1)/\omega_1$ is the detuning parameter, where ω_1 is the fundamental frequency.

Equation (9) has been solved numerically and the result was found to agree well with that obtained from simulation calculation for both waterbag and the Gaussian form of $F(R)$. The code used for the simulation calculation was TDA developed by Tran. and Wurtele [17]. The growth rate for the case of the Gaussian distribution function can be represented by the following simple interpolating formula:

$$\begin{aligned} \log \frac{\mu}{D} = & - (0.759 + 0.238\chi + 0.0139\chi^2) \\ & \times \left\{ 1 + \left(2k_1\epsilon_x \frac{k_\beta}{k_w D} \right)^2 \left(0.149 + 0.0268 \log \frac{k_\beta}{k_w D} \right) \right. \\ & \left. + (44.03 + 3.323\chi + 5.45\chi^2) \cdot \left[\left(\frac{\sigma_\gamma}{D} \right)^2 - 0.713 \left(\frac{\sigma_\gamma}{D} \right)^4 + 68.65 \left(\frac{\sigma_\gamma}{D} \right)^6 \right] \right\}^{1/2} \\ & ; \text{ for } 2k_1\epsilon_x \frac{k_w D}{k_\beta} \geq 0.05 \text{ and } \frac{k_\beta}{k_w D} \leq 1, \end{aligned} \quad (10.a)$$

and

$$\begin{aligned} \frac{\mu}{D} = & [0.0628 - 0.219\chi - 0.000568\chi^2]^{1/2} \\ & \exp \left[- \frac{\left(2k_1\epsilon_x \frac{k_\beta}{k_w D} \right)^2}{\left(1.091 + 0.1345 \frac{k_\beta}{k_w D} \right)} - (11.92 + 2.202\chi + 0.1414\chi^2) \cdot \left(\frac{\sigma_\gamma}{D} \right)^2 \right] \\ & ; \text{ for } 2k_1\epsilon_x \frac{k_w D}{k_\beta} < 0.05 \text{ or } \frac{k_\beta}{k_w D} > 1, \end{aligned} \quad (10.b)$$

where

$$D = 4 \sqrt{k k_u \Sigma \rho^3 / \pi} \text{ and } \chi = \log \left(2 k_1 \epsilon_x \frac{k_w D}{k_\beta} \right) .$$

In the above, D is a 3-D analogue of the Pierce parameter ρ [8]. Equation (10) enables us to calculate the growth rate quickly using a calculator rather than going through a full simulation calculation. Thus optimization of the growth rate with respect to several parameters can be carried out easily. An example is the optimization with respect to the betatron function β . For the natural focusing provided by an undulator, assuming that the focusing in the x plane is made equal to that in the y plane by shaping the pole [18], the β function is given by

$$\beta_x = \beta_y = \frac{K\pi}{\gamma \lambda_u} . \quad (11)$$

Often, a stronger focusing (for example, by employing external quadrupoles) than that provided by the natural focusing is desirable to increase the gain; A small value of β corresponds to a high density and therefore a large 1-D gain. However, when β becomes too small, the gain drops because of the increase in the effective energy spread as can be seen from Eq. (9). By studying the formula, Eq. (10), it was determined that the optimum value of β is roughly related to the minimum gain length as follows [19]:

$$\frac{1}{2 L_G} + 2 k_u \frac{\sigma_\gamma}{\gamma} = (2 k \epsilon_x)^{2/3} \frac{1}{\beta} . \quad (12)$$

4. Saturation

As the optical power build up, electrons are trapped and rotate in the phase space bucket. It is expected that the power growth will stop when the total accumulated synchrotron oscillation phase becomes about π , since the electrons will gain energy with further rotation [20]. Based on this observation, we can estimate the efficiency of SASE in converting the electron beam power into the optical power as follows: Let $\Omega(z)$ be the synchrotron oscillation frequency with the longitudinal distance z as the time. The condition that the saturation takes place at $z = L_s$ becomes

$$\int_0^{L_s} \Omega(z) dz = \pi . \quad (13)$$

Since Ω is proportional to $\sqrt{|A|}$, and $|A|$ increases exponentially as $\exp(k_u \mu z)$, the integral can be done with the following results:

$$\frac{\Omega(L_s) - \Omega(0)}{\frac{1}{2} k_u \mu} = \frac{\Omega(L_s)}{\frac{1}{2} k_u \mu} = \pi \quad (14)$$

This equation determines $|A|$ and therefore the optical energy density at saturation. Assuming that the cross sectional area of the optical beam is the same as that of the electron beam, the efficiency of the energy extraction can be written as follow [21]:

$$\eta = \frac{P_{sat}}{P_{el}} = \frac{\Omega^4(L_s)}{(4\rho)^3 k_u^4} , \quad (15)$$

where P_{sat} is the optical power at saturation, and P_{el} is the electron beam power. Inserting Eq. (14) into Eq. (15), we obtain

$$\eta = 0.86\rho \left(\frac{\mu}{\mu_{1D}} \right)^4 = \rho \left(\frac{\mu}{\mu_{1D}} \right)^4 , \quad (16)$$

where $\mu_{1D} = \sqrt{3} \rho$. Note that Eq. (16) reduces to $\eta \approx \rho$ for 1-D, cold beam limit in agreement with the previous result [1].

Actual efficiency calculated from simulation code appears to have a different functional dependence on μ from that given by Eq. (16); By carrying out simulation for a large number of cases, it is found that the efficiency can be represented by the following formula:

$$\eta \approx \rho \left(\frac{\mu}{\mu_{1D}} \right)^2 . \quad (17)$$

Figure (2) gives the plot of η/ρ for various cases and compare with Eq. (17). The agreement is good.

To estimate the length of the undulator L_s required for saturation, we assume that Eq. (2) is valid for $z = L_s$ and integrate over ω . Thus we obtain the following expression for the optical power at saturation P_{sat} :

$$P_{\text{sat}} = e^{L/L_G} \rho^2 \omega_1 E_0 / 2\pi \quad . \quad (18)$$

Here, we have used the fact that the bandwidth at saturation is about $\delta\omega/\omega \sim \rho$. From Eq. (18), we obtain

$$L_s = L_G \ln [P_{\text{sat}} (\omega_1 \rho^2 E_0 / 2\pi)] \quad . \quad (19)$$

It can be shown that the argument of the logarithm in the above is approximately the number of electrons in one coherence length $\ell_c = \lambda/\rho$ [3].

It may be possible to introduce a tapered undulator after saturation of SASE to extract more power [22]. However, the radiation bandwidth at saturation is comparable to the bucket height, and thus the position of the bucket becomes ambiguous. Therefore, it may not be possible to trap a sufficient number of electrons and displace it downward in the electron phase space. This point needs to be investigated carefully.

5. Accelerator System For SASE

In Eq. (19), logarithmic factor is typically about 10 in our examples. In order to limit L_s to a reasonable length, it is important to avoid any significant reduction in gain (thus minimizing L_G) by satisfying the conditions (6), (7) and (8). Thus, very tight requirements must be satisfied on electron beam characteristics to achieve short wavelength SASE. In the following, we discuss accelerator systems producing the required electron beams.

5.1 Storage Rings

Storage rings provide high-brightness electron beams because of the radiation damping mechanism [23]. A scheme for producing SASE in a special by-pass of a storage ring was proposed by C. Pellegrini [2]. In this scheme, an electron bunch, which is normally circulating in the main storage ring, is directed into a special by pass section where it interacts with a long undulator to produce SASE. The electron bunch is then routed back to the ring to recover the

beam qualities degraded by the FEL interaction. The technology to build high-brightness storage rings has been progressed considerably recently due to the synchrotron radiation source construction at several places around the world. Detailed study of accelerator physics for a storage ring/by-pass system for SASE was carried out in reference [11].

Designing a storage ring/by-pass system suitable for SASE involves a complicated optimization between various limiting effects. Thus, in order to achieve small emittance, the ring should consist of a large number of bending sections to minimize the quantum fluctuation due to synchrotron radiation. Such a ring tends to have a small momentum compaction, and has therefore a lower microwave instability threshold, giving rise to an increase in the bunch length and the energy spread. Also, high current density required for high gain leads to an increase in the phase space volume due to the intrabeam scattering. With the examples worked out so far, it appears that SASE in storage rings is possible for wavelengths longer than several hundred Angstroms.

The average power produced by a storage ring based SASE is limited by the Renieri limit [24]. In the present context, the limit is about ρP_{syn} , where P_{syn} is the synchrotron radiation power emitted in the main ring. This is another drawback for the storage ring based SASE for applications requiring high average power.

5.2 Linacs

The brightness of the electron beams in a linac is limited by that of the injector, which prepares properly bunched electron beams for RF acceleration. With the traditional injectors based on thermionic gun and bunchers, it has been difficult to produce electron beams of sufficiently high brightness due to phase space dilution in the bunching process. Recently, a new type of injector based on RF photocathode concept [13] is being developed at LANL and other laboratories that overcomes the buncher problem. With the RF photocathode gun, the linacs become an attractive option for short wavelength SASE.

The beam dynamics in RF photocathode has been studied by a simple model [25]. The electron beam emittances due to space charge effect ϵ_x^{sc} and due to the RF effect ϵ_x^{rf} are estimated to be

$$\gamma \epsilon_x^{sc} = \left(\frac{2mc^2}{eE} \right) \frac{I}{I_A} \frac{1}{(3\sigma_x/\sigma_z + 5)} , \quad (22.a)$$

$$\gamma \epsilon_x^{rf} = \frac{eE}{2\sqrt{2} mc^2} \left(\frac{2\pi}{\lambda_{RF}} \right)^2 \sigma_x^2 \sigma_z^2 , \quad (22.b)$$

where E is the accelerating gradient, I is the electron beam current, I_A is the Alfvén current (17000 A), σ_x and σ_z are the transverse and longitudinal beam sizes, and λ_{RF} is the RF wavelength. With E about 100 MV/m, and $\sigma_x/\sigma_z \geq 5$, the normalized emittance estimated from Eq. (22.a) for $I \sim 100$ -200 A is a few mm-mrad. The emittance due to the RF effect, Eq. (22.b), is negligible. Since the emittance decreases as $1/\gamma$ with acceleration, such a beam after acceleration to several GeV can be used for an SASE driver for wavelengths shorter than 100 Å. For a high gain, the peak current needs to be increased by an order of magnitude, and this can be done by magnetic bunching. Throughout the process of acceleration, transport and bunching of the electron beam, various phase space dilutions due to longitudinal and transverse wakefields, RF deflections, and dispersive errors, etc., need to be carefully controlled. The technology of acceleration and bunching while preserving the emittance has been developed extensively in connection with the recent linear collider projects.

An Example of a 4 nm SASE based on SLAC linac being proposed by SLAC/SSRL/UCLA/LBL collaboration [12] is given in Table 1. Here, a section of the SLAC linac accelerates electron beam produced from a photo-injector. Longitudinal bunch compression at intermediate energies increases the peak current tenfold to 2.5 kA. Two cases are considered, one with 3.5 GeV and one with 7 GeV electron beams. The lower energy case produces somewhat less power but in a shorter distance. The gain in these examples are maximized by choosing an appropriate focusing, roughly in accordance with Eq. (12), in order to keep the undulator length to about 50 m. Therefore an external focusing elements, such as quadrupoles, are required. The saturated SASE output power for both cases is in the

multigigawatt range, producing about 10^{14} coherent photons in a pulse. Such an output will permit imaging a biological sample in a single subpicosecond pulse.

References

- [1] R. Bonifacio, C. Pellegrini and L. M. Narducci, Opt. Commun. 50, 373 (1984).
- [2] C. Pellegrini, Journ. Opt. Soc. Amer., B2, 259 (1985).
- [3] K.-J. Kim, Nucl. Instr. Meth., A250, 396 (1986).
- [4] J.-M. Wang and L.-H. Yu, Nucl. Instr. Meth., A250, 484 (1986).
- [5] G.T. Moore, Nucl. Instr. Meth., A239, 19(1985).
- [6] E.T. Scharlemann, A.M. Sessler, and J.S. Wurtele, Phys. Rev. Lett. 54, 1925 (1985).
- [7] K.-J. Kim, Phys. Rev. Lett., 57, 1871 (1986).
- [8] L.-H. Yu, S. Krinsky and R. Gluckstern, Phys. Rev. Lett., 64, 3011 (1990).
- [9] Y.-H. Chin, K.-J. Kim and M. Xie, Nucl. Instr. Meth., A318, 481 (1992); "Three-Dimensional Theory of Small-Signal, High-Gain Free Electron Laser Including Betatron Oscillations," to be published in Phys. Rev. A; "Calculation of 3-D Free Electron Laser Gain: Comparison with Simulation and Generalization to Elliptical Cross Section," LBL-32286, these proceedings.
- [10] T.J. Orzechowski et al., Phys. Rev. Lett. 54, 889 (1985).
- [11] K.-J. Kim et al., Nucl. Instr. Meth. A239, 54 (1985); J. Bisognano et al., Part. Accel., Vol. 18, 223 (1986); C. Pellegrini, Nucl. Instr. Meth., A272, 364 (1988).
- [12] C. Pellegrini et al., "A 2 to 4 nm High Power FEL on the SLAC Linac," Paper submitted to 13 FEL Conf.
- [13] R. L. Sheffield, in Physics of Particle Accelerators, AIP Vol. 184, 1500, M. Month and M. Dienes eds., (1989).
- [14] L.-H. Yu and S. Krinsky, Nucl. Instr. Meth., A285, 119 (1989).
- [15] K.-J. Kim, Nucl. Instr. Meth., A246, 71 (1986).
- [16] C. Pellegrini, Nucl. Instr. Meth. A239, 127 (1985).

- [17] T.M. Tran and J.S. Wurtele, Comput. Phys. Comm. 54, 263 (1989).
- [18] E.T. Scharlemann, Journ. Applied Phys. 58, 2154 (1985).
- [19] Y.-H. Chin, "Simple Formulae for the Optimization of the FEL Gain Length Including the Effects of Emittance, Betatron Oscillations and Energy Spread," these proceedings.
- [20] Such an argument was apparently well-known to the pioneers of the electron devices. See, for example, J.C. Slater, "Microwave Electronics" (Van Nostrand, Princeton, 1950), page 297-298. We thank Henry Freund for pointing this out.
- [21] L.-H. Yu, Phys. Rev. A44, 5178 (1991).
- [22] K.-J. Kim, in Workshop on Fourth Generation Light Sources, SSRL Report 92/02, page 315, M. Cornacchia and H. Winick, eds. (1992).
- [23] See for example, M. Sands, "Physics of Electron Storage Rings," SLAC-121 (1970).
- [24] A. Renieri, Nuovo Cimento 53B, 160 (1979).
- [25] K.-J. Kim, Nucl. Instr. Meth. A275, 201 (1989).

Table 1

Parameter for 4 nm SASE based on SLAC Linac

ELECTRON BEAM PROPERTIES

Energy, GeV	7	3.5
Emittance, normalized, rms, mm-mrad	3	3
Peak Current, A	2,500	2,500
Uncorrelated Energy Spread, rms, %	0.04	0.07
Correlated Energy Spread, rms, %	0.1	0.1

UNDULATOR PROPERTIES

Period, cm	8.3	5
Magnetic field, T	0.78	0.8
Undulator parameter	6	3.7
Focusing β , m	10	5

FEL PROPERTIES

Wavelength, nm	4	4
Power Gain Length, m	3.4	2.6
Undulator Saturation Length, m	60	48
Peak Power at Saturation, GW	28	10
Pulse Duration, rms, ps	0.16	0.16
Line width, rms, including chirping, %	0.2	0.2
Photons per Pulse	2.7×10^{14}	1×10^{14}
Energy per Pulse, mJ	11	4
Peak Brightness, Ph/mm ² /mrad ²	3.6×10^{31}	0.8×10^{31}
Repetition Rate, Hz	120	120
Average Power, W	1.2	0.5
Average Brightness, Ph/mm ² /mrad ²	3.6×10^{21}	1.3×10^{21}

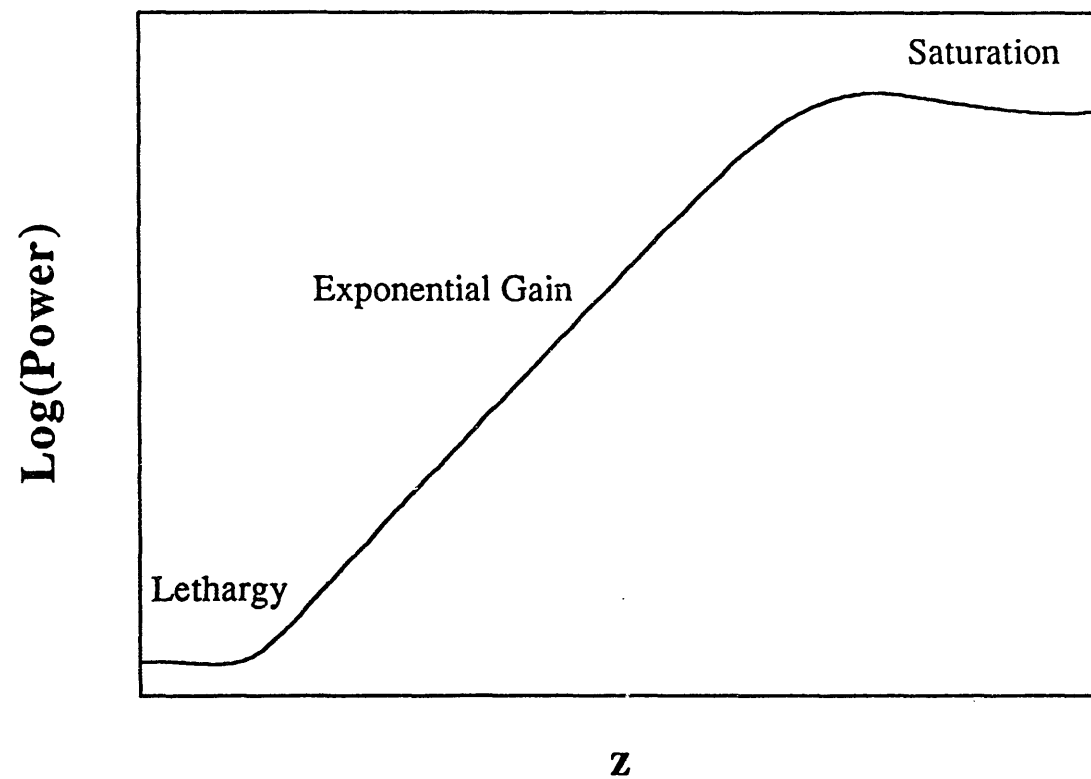


Fig. 1 Schematic representation of FEL power growth vs. interaction length.

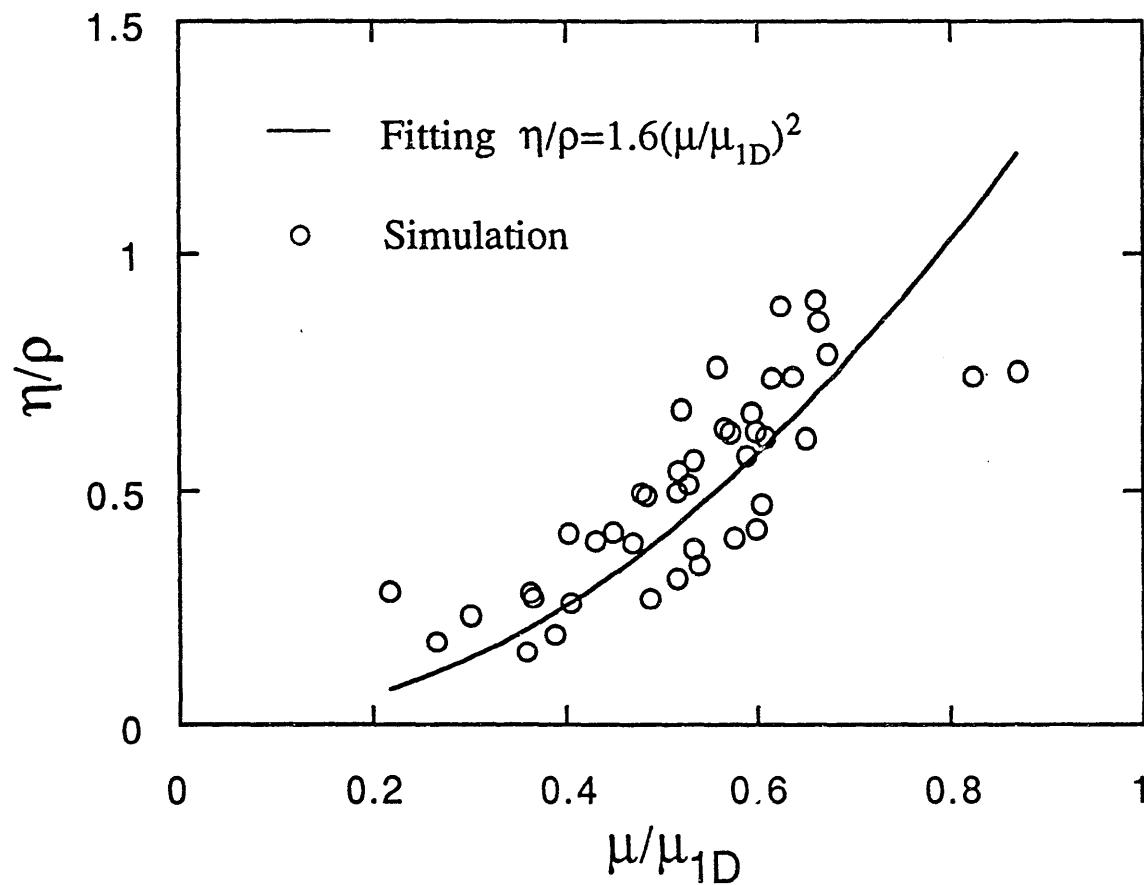


Fig. 2 Simulation results of the FEL efficiency divided by Pierce parameter vs. the FEL growth rate divided by its 1D value, and quadratic fitting of the data.